J. Fluid Mech. (1984), *vol.* 146, *pp.* 1–20
Printed in Great Britain

Oblique wave groups in deep water

By P. J. BRYANT
Mathematics Department, University of Canterbury, Christchurch, New Zealand

(Received 17 November 1982 and in revised form 6 April 1984)

Oblique wave groups consist of waves whose straight parallel lines of constant phase are oblique to the straight parallel lines of constant group phase. Numerical solutions for periodic oblique wave groups with envelopes of permanent shape are calculated from the equations for irrotational three-dimensional deep-water motion with nonlinear upper free-surface conditions. Two distinct families of periodic wave groups are found, one in which the waves in each group are in phase with those in all other groups, and the other in which there is a phase difference of π between the waves in consecutive groups. It is shown that some analytical solutions for oblique wave groups calculated from the nonlinear Schrödinger equation are in error because they ignore the resonant forcing of certain harmonics in two dimensions. Particular attention is given to oblique wave groups whose group-to-wave angle is in the neighbourhood of the critical angle $\tan^{-1}\surd\frac{1}{2}$, corresponding to waves on the boundary wedge of the Kelvin ship-wave pattern.

1. Introduction

When waves are generated over a range of horizontal directions, it must be expected that the lines of constant wave phase in a locally sinusoidal group of waves are oblique to the lines of constant phase of the envelope enclosing the group. One well-known example is that of the waves along the boundary wedge of the Kelvin ship-wave pattern (Lighthill 1978, figures 70, 71). Another example results from the instability of finite-amplitude deep-water gravity waves to disturbances in two horizontal dimensions. An oblique unstable modulation of a length large compared with the wavelength causes a regular wavetrain to grow into an oblique wave-group structure. Such oblique instabilities dominate parallel instabilities for moderate and large wave steepnesses (McLean *et al.* 1981).

A simple description of a periodic oblique wave group is given by the superposition of two sinusoidal waves differing slightly in wavenumber components along one horizontal direction. Their water surface displacement may be represented by

$$\eta(x_1,x_2,t) = a\cos\{k_1x_1+k_2x_2-\omega t\}+a\cos\{(k_1+\delta k_1)\,x_1+k_2x_2-(\omega+\delta\omega)\,t\} \quad (1.1a)$$

$$= 2a\cos\{\tfrac{1}{2}\delta k_1x_1-\tfrac{1}{2}\delta\omega t\}\cos\{(k_1+\tfrac{1}{2}\delta k_1)\,x_1+k_2x_2-(\omega+\tfrac{1}{2}\delta\omega)\,t\}, \quad (1.1b)$$

where $\omega = (g\kappa)^{\frac{1}{2}}$, $\kappa = (k_1^2+k_2^2)^{\frac{1}{2}}$, and ω is the frequency of waves in deep water. This superposition describes a slowly varying wavetrain propagating at angle θ to the x_1 direction, where $\tan\theta = k_2/k_1$ approximately, whose group envelope propagates in the x_1 direction with a velocity approximately

$$\frac{\partial\omega}{\partial k_1} = \frac{1}{2}\left(\frac{g}{\kappa}\right)^{\frac{1}{2}}\cos\theta. \quad (1.2)$$

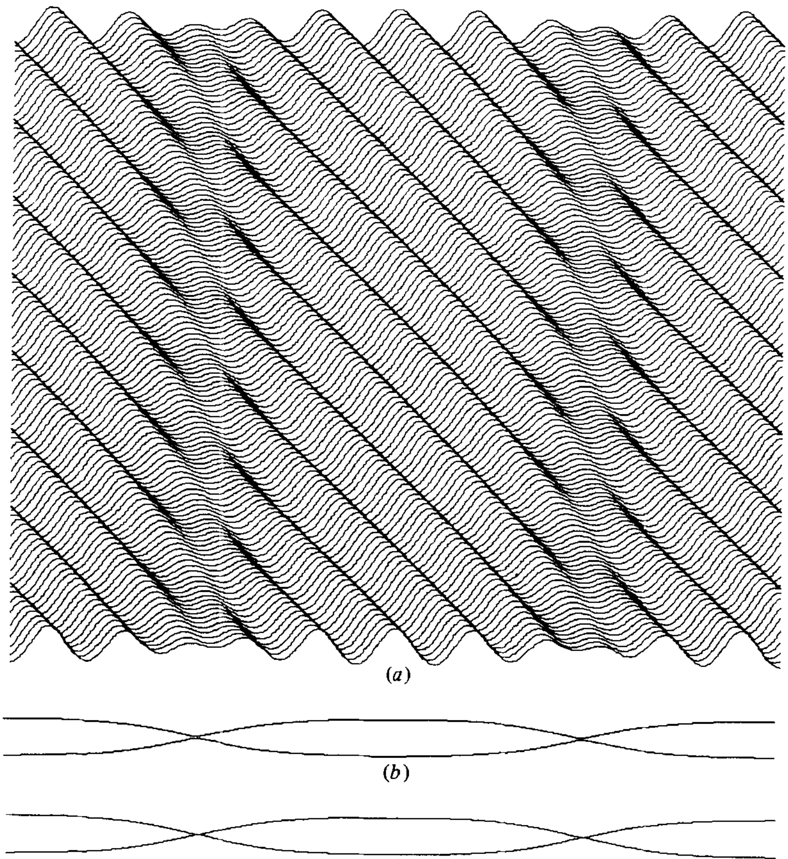

(a)

(b)

(c)

FIGURE 1. (a) Two group lengths of the oblique wave group with parameters $\epsilon = 0.05$, $k_0 = 10$, $\theta = \frac{1}{4}\pi$, of the second family above the critical angle. Note the phase shift of π between the crest lines of consecutive groups. Horizontal contraction 10π. (b) Envelope of the above groups. Minimum separation of upper and lower envelopes is 0.083 of maximum separation. (c) Corresponding envelope solution (sn form) of the nonlinear Schrödinger equation.

A generalization of this description is

$$\eta(x_1, x_2, t) = \sum_{k_1} a(k_1) \cos\{k_1 x_1 + k_2 x_2 - \omega t\}, \tag{1.3}$$

whose spectrum lies in a narrow waveband centred on wavenumber (k_0, k_2) for fixed k_2, and ω is dependent on group amplitude as well as on k_1 and k_2.

An example of an oblique wave group structure for which $\theta = \frac{1}{4}\pi$ is sketched in figure 1(a). The wavetrain propagates towards the top right of the figure with a velocity $(g/\kappa)^{\frac{1}{2}}$, while the group structure propagates from left to right with a velocity $\frac{1}{2}(g/\kappa)^{\frac{1}{2}} \cos\frac{1}{4}\pi$. At the small value of the wave-slope parameter $\epsilon = 0.05$ in the figure, the main effect of the weak nonlinearity is to maintain the permanent envelope shape by balancing the linear dispersion.

A simple representation of a one-dimensional wave-group structure is

$$\eta = \sum_k a_k \cos\frac{kx}{k_0} \tag{1.4a}$$

$$= \sum_k a_k \cos\left(\frac{k-k_0}{k_0}x + x\right), \tag{1.4b}$$

where the wavenumbers k take all integer values in a waveband centred on k_0, and the amplitudes a_k rise to a maximum at or near k_0 (k_0 need not be an integer). The envelope of this group is

$$\eta_{\mathrm{E}} = \left\{\left(\sum_k a_k \cos\frac{k-k_0}{k_0}x\right)^2 + \left(\sum_k a_k \sin\frac{k-k_0}{k_0}x\right)^2\right\}^{\frac{1}{2}} \tag{1.5a}$$

$$= \left\{\sum_k a_k^2 + \sum_l \sum_{\substack{m \\ l \neq m}} a_l a_m \cos\frac{l-m}{k_0}x\right\}^{\frac{1}{2}}. \tag{1.5b}$$

The envelope has group length $2\pi k_0$ and encloses a wavetrain of approximate wavelength 2π. An alternative wave-group structure is that for which the wavenumbers k in (1.4, 1.5) take all odd integer values in a waveband centred on k_0. The envelope described by (1.5) then has group length πk_0, and from (1.4) encloses a wavetrain of approximate wavelength 2π. Each wavetrain satisfies

$$\eta(x+2\pi k_0) = \eta(x), \tag{1.6a}$$

and for the second family only,

$$\eta(x+\pi k_0) = -\eta(x). \tag{1.6b}$$

The wavetrains in each group of the first family are in phase, but the wavetrains in consecutive groups of the second family are π out of phase. The two families are generalized in §5 to oblique wave-group structures in the horizontal plane with harmonic wavebands included.

Hui & Hamilton (1979) calculated oblique wave-group solutions from the nonlinear Schrödinger equation in two horizontal dimensions. This equation, derived originally by Zakharov (1968), assumes that the spectrum of surface waves rises to a narrow central peak in two-dimensional wavenumber space. The wave frequencies are expanded in a Taylor series about the central wavenumber, with the leading terms of the series contributing the linear terms to the nonlinear Schrödinger equation. If resonances cause further significant peaks in the spectrum of water waves, the Taylor-series expansion is not valid, and the nonlinear Schrödinger equation fails as a model equation for the wave-group structure. It will be shown that resonances are either absent or insignificant for oblique wave groups whose group-to-wave angle is less than about $\tan^{-1}\frac{1}{2}$, but that for greater angles, including the important critical angle $\tan^{-1}\sqrt{\frac{1}{2}}$, resonances can be significant even to the extent at some angles that they dominate the oblique wave group structure.

The nonlinear Schrödinger equation has oblique wave-group solutions for which the envelope of the group passes through zero (Hui & Hamilton 1979, figures 2 and 3). No numerical solutions of the full equations were found with envelope zeros. Solutions of the full equations corresponding to such Schrödinger-equation solutions have upper and lower envelope extrema where the Schrödinger-equation solutions have envelope zeros (figures 1 *b*, *c*). Further, it was found that solutions of the second family corresponded to Schrödinger-equation solutions with envelope zeros, with the discontinuity in wave phase of π at an envelope zero replaced by a phase shift of π between the wavetrains in consecutive wave groups.

2. Oblique wave groups

The set of equations governing gravity waves in inviscid irrotational motion on the surface of deep water is

$$\phi_{xx}+\phi_{yy}+\phi_{zz}=0 \quad (z<\epsilon\eta(x,y,t)), \tag{2.1a}$$

$$\phi_x, \phi_y, \phi_z \to 0 \quad \text{as} \quad z\to-\infty, \tag{2.1b}$$

$$\eta_t-\phi_z+\epsilon\eta_x\phi_x+\epsilon\eta_y\phi_y=0 \quad (z=\epsilon\eta(x,y,t)), \tag{2.1c}$$

$$\eta+\phi_t+\tfrac{1}{2}\epsilon(\phi_x^2+\phi_y^2+\phi_z^2)=0 \quad (z=\epsilon\eta(x,y,t)). \tag{2.1d}$$

The dimensional variables are the surface displacement $a\eta$, the velocity potential $(gl)^{\frac{1}{2}}a\phi$, and lx, ly, lz, $(l/g)^{\frac{1}{2}}t$, where a is a measure of wave amplitude, $2\pi l$ is a typical wavelength, and $\epsilon = a/l$ is a measure of wave steepness. The origin of coordinates lies in the mean water surface, with the z-axis vertically upwards.

A non-dimensional description of a simple periodic oblique wave group with an envelope of permanent shape is, from (1.3, 1.4),

$$\eta = \sum_k a_k \cos\left\{\frac{k}{k_0}x\cos\theta+y\sin\theta-\omega t\right\} \tag{2.2a}$$

$$= \sum_k a_k \cos\left\{\frac{k-k_0}{k_0}(x-\tfrac{1}{2}t\cos\theta)\cos\theta+x\cos\theta+y\sin\theta-(1+\alpha)t\right\}, \tag{2.2b}$$

which describes a slowly varying wavetrain of typical wavelength $2\pi l$ propagating at angle θ to the x-direction, whose group envelope propagates with velocity $\frac{1}{2}\cos\theta(gl)^{\frac{1}{2}}$ in the x-direction. The dimensional wavenumber components in the x-direction are k/L, where $2\pi L$ is the group length. The central wavenumber component in this direction is k_0/L, such that

$$k_0 = \frac{L\cos\theta}{l} \tag{2.3}$$

is equal to or is near to the number of wavelengths in one group length in the x-direction for the first family or two group lengths for the second family (k_0 is identified with the central peak of the spectrum and is not required to be an integer, although k takes only integer values). The nonlinear amplitude dependence of the wavetrain is reflected in a non-dimensional frequency contribution α, an unknown function of ϵ, k_0 and θ.

A complete representation of an oblique periodic wave group including harmonic wavebands centred on jk_0, $j=0,1,2,\ldots$, where $j=1$ denotes the dominant waveband, is given by

$$\eta = \sum_{j=0}^{J}\sum_{k=k_1(j)}^{k_2(j)} a_{jk}\cos\left\{\frac{k-jk_0}{k_0}(x-\tfrac{1}{2}t\cos\theta)\cos\theta+j(x\cos\theta+y\sin\theta-(1+\alpha)t)\right\}. \tag{2.4a}$$

The bounds of the summations are determined numerically by trial and error so that the set of amplitudes a_{jk} includes all those amplitudes greater in magnitude than some small prescribed value. Since η is chosen to have a zero mean and the argument is symmetric in k when $j=0$, the lower bound $k_1(0)$ may be set equal to 1 without loss of generality. Other lower bounds $k_1(j)$, $j>0$, may be negative. The associated solution of Laplace's equation (2.1 a) is

$$\phi = \sum_{j=0}^{J}\sum_{k=k_1(j)}^{k_2(j)} b_{jk}\,e^{\kappa_{jk}z}\sin\left\{\frac{k-jk_0}{k_0}(x-\tfrac{1}{2}t\cos\theta)\cos\theta+j(x\cos\theta+y\sin\theta-(1+\alpha)t)\right\}, \tag{2.4b}$$

where
$$\kappa_{jk} = \left\{\left(\frac{k\cos\theta}{k_0}\right)^2 + (j\sin\theta)^2\right\}^{\frac{1}{2}}.$$

It should be emphasized that (2.4*a*, *b*) are only one particular description of periodic oblique wave groups, and are a generalization of the two families of wave groups modelled by (1.4–1.6). Further periodic wave-group solutions can be expected to exist with the greater degree of generality allowed by writing (2.4*a*) with both a set of amplitudes a_{jk} and a set of phases θ_{jk} not all zero. Equations (2.4*a*, *b*) are numerically complete in the sense that they include a complete set of wave components, greater in magnitude than some small prescribed value, which are generated by the nonlinear interactions described by (2.1*c*, *d*).

When (2.4*a*, *b*) are substituted into (2.1*c*, *d*), with c_{jk} denoting the cosine in (2.4*a*) and s_{jk} the sine in (2.4*b*), the resulting expressions may be written as

$$\begin{aligned} F = \sum_j\sum_k &\left\{\left[j(1+\alpha-\tfrac{1}{2}\cos^2\theta)+\frac{k}{2k_0}\cos^2\theta\right]a_{jk}s_{jk}-\kappa_{jk}b_{jk}\,\mathrm{e}^{\epsilon\kappa_{jk}\eta}\,s_{jk}\right\} \\ &-\epsilon\left(\sum_j\sum_k\frac{k}{k_0}\cos\theta\, a_{jk}s_{jk}\right)\left(\sum_j\sum_k\frac{k}{k_0}\cos\theta\, b_{jk}\,\mathrm{e}^{\epsilon\kappa_{jk}\eta}\,c_{jk}\right) \\ &-\epsilon\,(\sum_j\sum_k j\sin\theta\, a_{jk}s_{jk})\,(\sum_j\sum_k j\sin\theta\, b_{jk}\,\mathrm{e}^{\epsilon\kappa_{jk}\eta}\,c_{jk}) = 0, \end{aligned} \tag{2.5a}$$

$$\begin{aligned} G = \sum_j\sum_k &\left\{a_{jk}c_{jk}-\left[j(1+\alpha-\tfrac{1}{2}\cos^2\theta)+\frac{k}{2k_0}\cos^2\theta\right]b_{jk}\,\mathrm{e}^{\epsilon\kappa_{jk}\eta}\,c_{jk}\right\} \\ &+\tfrac{1}{2}\epsilon\left(\sum_j\sum_k\frac{k}{k_0}\cos\theta\, b_{jk}\,\mathrm{e}^{\epsilon\kappa_{jk}\eta}\,c_{jk}\right)^2+\tfrac{1}{2}\epsilon\left(\sum_j\sum_k j\sin\theta\, b_{jk}\,\mathrm{e}^{\epsilon\kappa_{jk}\eta}\,c_{jk}\right)^2 \\ &+\tfrac{1}{2}\epsilon\left(\sum_j\sum_k \kappa_{jk}b_{jk}\,\mathrm{e}^{\epsilon\kappa_{jk}\eta}\,s_{jk}\right)^2 = 0, \end{aligned} \tag{2.5b}$$

where $\mathrm{e}^{\epsilon\kappa_{jk}\eta} = \exp\,(\epsilon\kappa_{jk}\Sigma_p\Sigma_q\, a_{pq}c_{pq})$. If the measure of amplitude a is taken to be the water-surface displacement $\eta(0,0,0)$ then

$$H = \sum_j\sum_k a_{jk}-1 = 0. \tag{2.5c}$$

Equations (2.5*a*, *b*) may be transformed numerically to

$$F = \sum_m\sum_n F_{mn}s_{mn} = 0, \quad G = \sum_m\sum_n G_{mn}c_{mn} = 0, \tag{2.6a, b}$$

from which
$$F_{mn} = G_{mn} = 0 \quad \text{for all } m,n. \tag{2.7}$$

Equations (2.6) are obtained from (2.5) for given values of a_{jk}, b_{jk} (all j and k) and α by evaluating F and G at a grid of points in space and time followed by fast Fourier transforms over the grid. The independent variables used for the grid are the multipliers of j and k in the phase functions defined by (2.4). This process, using truncated Fourier series, does not need perturbation expansions in ϵ and makes no explicit assumptions about the magnitude of ϵ.

The Fourier coefficients F_{mn}, G_{mn} are nonlinear functions of a_{jk}, b_{jk} (all j and k) and α for given ϵ, k_0 and θ. Equations (2.7) are solved numerically by Newton's method, which for F is given by

$$\sum_j\sum_k\left(\frac{\partial F}{\partial a_{jk}}\right)_{mn}(a_{jk}-a'_{jk})+\sum_j\sum_k\left(\frac{\partial F}{\partial b_{jk}}\right)_{mn}(b_{jk}-b'_{jk})+\left(\frac{\partial F}{\partial \alpha}\right)_{mn}(\alpha-\alpha') = F_{mn} \tag{2.8}$$

for all m, n. Each coefficient on the left of (2.8) is an (m, n) Fourier coefficient of a partial derivative of (2.5a), and is calculated numerically by the method described above for calculating F_{mn}, G_{mn}. The prime denotes the new value of each variable. All Fourier coefficients are evaluated at the old values of the variables. There is a similar set of equations derived from G and a single equation derived from H. The complete set of linear equations is solved numerically for $a_{jk}-a'_{jk}$, $b_{jk}-b'_{jk}$ (all j and k), $\alpha-\alpha'$, the new values of the variables are calculated, and the procedure is repeated until the differences are less than some small arbitrary number (10^{-6} or 10^{-8} in the examples following). This method is the same as that used previously for the calculation of cyclic waves in one horizontal dimension, those being waves for which the group length equals the wavelength (Bryant 1983).

A useful feature of the numerical method is that the Fourier coefficients F_{mn}, G_{mn} may be found for wavebands m and wavenumbers n outside those included in the calculation of a_{jk}, b_{jk} (all j and k) and α. These coefficients then show which wavebands and wavenumbers should be added to the calculation to improve the precision with which (2.6a, b) are satisfied over the complete range of x, y and t. All calculations were performed in double precision on a Prime 750 computer, with subroutines adapted from the Harwell Subroutine Library.

3. Nonlinear Schrödinger equation

The nonlinear Schrödinger equation describing wave propagation in the x-direction on deep water, with the same dimensional scaling as in §2, is

$$\mathrm{i}(A_t+\tfrac{1}{2}A_x)-\tfrac{1}{8}A_{xx}+\tfrac{1}{4}A_{yy}-\tfrac{1}{2}\epsilon^2\,|A|^2A=0, \tag{3.1}$$

where the non-dimensional surface displacement is

$$\eta=\mathrm{Re}\,\{A(X,\,Y,t)\exp\mathrm{i}(X-t)\}, \tag{3.2}$$

and A is a slowly varying function of X, Y, and t. Oblique wave-group solutions of the form described by (2.2) require the rotation of axes

$$x=X\cos\theta-Y\sin\theta,\quad X=x\cos\theta+y\sin\theta,$$

$$y=X\sin\theta+Y\cos\theta,\quad Y=-x\sin\theta+y\cos\theta,$$

followed by substitution in (3.1) of

$$A=R(x-\tfrac{1}{2}t\cos\theta)\,\mathrm{e}^{-\mathrm{i}\alpha t}. \tag{3.3}$$

The function R is found to satisfy

$$(\cos^2\theta-2\sin^2\theta)\,R''-8\alpha R+4\epsilon^2R^3=0, \tag{3.4}$$

which is the equation whose analytical solutions are derived by Hui & Hamilton (1979, equation 16).

The dominant waveband of the surface displacement described by (2.4a) is

$$\sum_{k=k_1(1)}^{k_2(1)} a_{1k}\cos\left\{\frac{k-k_0}{k_0}(x-\tfrac{1}{2}t\cos\theta)\cos\theta\right\}\cos(X-(1+\alpha)\,t)$$

$$-\sum_{k=k_1(1)}^{k_2(1)} a_{1k}\sin\left\{\frac{k-k_0}{k_0}(x-\tfrac{1}{2}t\cos\theta)\cos\theta\right\}\sin(X-(1+\alpha)\,t)$$

$$=S\cos(X-(1+\alpha)\,t)-T\sin(X-(1+\alpha)\,t) \tag{3.5a}$$

$$=R\cos(X-(1+\alpha)\,t+\Theta). \tag{3.5b}$$

where S, T, R, and Θ are functions of $x-\frac{1}{2}t\cos\theta$, with $S = R\cos\Theta$ and $T = R\sin\Theta$. The oblique wave-group solutions of the nonlinear Schrödinger equation are recovered only if Θ is assumed to be a linear function of $x-\frac{1}{2}t\cos\theta$ (Hui & Hamilton 1979, equation 9). This is equivalent to assuming that the total wave phase $X-(1+\alpha)t+\Theta$ has no dependence on $x-\frac{1}{2}t\cos\theta$ for any given wavetrain, because the linear dependence of Θ on x and t may be incorporated with $X-(1+\alpha)t$ by a suitable rescaling. The present representation of the dominant waveband is more general therefore than that assumed in oblique wave-group solutions of the nonlinear Schrödinger equation, since it provides for nonlinear dependence of Θ on $x-\frac{1}{2}t\cos\theta$.

Equation (3.4) may be solved numerically by a simplified version of the method described in §2. The Fourier-series expansion for R that is consistent with (3.5) with Θ scaled to zero is

$$R = \sum_k a_k \exp \mathrm{i}\left\{\frac{k-k_0}{k_0}(x-\tfrac{1}{2}t\cos\theta)\cos\theta\right\}, \tag{3.6}$$

where a_k is symmetric about $k = k_0$ (k_0 must be an integer here, since the non-dimensional wavelength is exactly 2π when $\Theta = 0$). When (3.6) is substituted into (3.4) the result may be transformed numerically to

$$G = \sum_m G_m \exp \mathrm{i}\left\{\frac{m-k_0}{k_0}(x-\tfrac{1}{2}t\cos\theta)\cos\theta\right\} = 0, \tag{3.7}$$

where G_m is symmetric about $m = k_0$, and is a nonlinear function of a_k and α for given ϵ, k_0 and θ. The Fourier transforms of the partial derivatives $(\partial G/\partial a_k)_m$, $(\partial G/\partial \alpha)_m$ are calculated, and Newton's method based on equations similar to (2.8) is used with the same procedure as was described in §2. All of the types of periodic solution derived by Hui & Hamilton (1979) have been calculated by this method.

4. Critical angle and conjugate solutions

The boundary wedge of the Kelvin ship-wave pattern is a caustic with oblique wave-group structure, according to the linear theory, for which the wave-crest to group-crest angle is the critical angle $\tan^{-1}\sqrt{\frac{1}{2}}$, equal to 0.6155 or 35.3°. The water-surface displacement on the boundary wedge dominates asymptotically the surface displacement within the wedge. The linear theory is summarized by Hui & Hamilton (1979, §4) and is illustrated by Lighthill (1978, figures 70, 71).

The nonlinear oblique wave-group solutions described in §2 were explored by changing θ step by step with ϵ and k_0 held constant. Solution branches followed in this way were liable to change either continuously or discontinuously to solution branches with the correct envelope velocity and correct wavelength in the y-direction, but with an incorrect wavelength in the x-direction, equivalent to an incorrect value of k_0. This meant that the chosen scaling was incorrect, and that such solutions needed rescaling, as follows.

If $2\pi l'$ denotes the correct typical wavelength of the wavetrain in its direction of propagation, and θ' is the correct angle between the propagation direction and the x-direction, the envelope velocity is

$$\tfrac{1}{2}(gl)^{\frac{1}{2}}\cos\theta = \tfrac{1}{2}(gl')^{\frac{1}{2}}\cos\theta' \tag{4.1}$$

in the x-direction, and the wavelength in the y-direction is

$$\frac{2\pi l}{\sin\theta} = \frac{2\pi l'}{\sin\theta'}. \tag{4.2}$$

Equation (2.3) becomes

$$k_0' = \frac{L\cos\theta'}{l'},$$

giving the correct number of wavelengths per group length in the x-direction. When the ratio l'/l is eliminated between (4.1) and (4.2), and the solution $\theta' = \theta$ discarded, θ and θ' are related by

$$\sin^2\theta + \sin\theta'\sin\theta + \sin^2\theta' = 1. \tag{4.3}$$

Knowing that the critical angle is $\sin^{-1}\surd\frac{1}{3}$, (4.3) may be rewritten

$$(1-3\sin^2\theta')(3\sin^2\theta - 1) = (3\sin\theta\sin\theta' + 2)(\sin\theta - \sin\theta')^2. \tag{4.4}$$

The right-hand side of this equation is greater or equal to zero for θ and θ' both positive acute angles, and is equal to zero only when

$$\theta = \theta' = \sin^{-1}\surd\tfrac{1}{3}.$$

Equation (4.4) shows that, if an oblique wave-group solution exists whose wave-crest to group-crest angle satisfies $\sin\theta > \surd\frac{1}{3}$, there is a conjugate oblique wave-group solution whose wave-crest to group-crest angle satisfies $\sin\theta' < \surd\frac{1}{3}$, and *vice versa*. The solution at the critical angle $\sin^{-1}\surd\frac{1}{3}$ is conjugate to itself. Conjugate solutions have the same envelope velocity and the same wavelength transverse to the direction of the envelope velocity, but have different wavelengths along the direction of the envelope velocity. Their occurrence is discussed in §6 in the context of wave resonance.

5. Two families of wave groups

It was shown in §1 how a single-waveband model of a periodic wave group possesses two distinct forms, one in which the waves in each group are in phase with those in all other groups, and the other in which there is a phase difference of π between the waves in consecutive groups. This property may be generalized to the oblique wave groups described by (2.4). For the first family, k takes all integer values between the bounds $k_1(j)$, $k_2(j)$ for each waveband j, while, for the second family, k takes only integer values such that $j+k$ is even. The second family for the simple model in §1 was described by the dominant waveband $j = 1$ with k taking odd values only.

The oblique wave groups propagate in the x-direction with a dimensionless group length $2\pi k_0/\cos\theta$ equivalent to a dimensional group length $2\pi L$ (equation 2.3). Both families of oblique wave groups (equation 2.4a) satisfy

$$\eta\left(x+\frac{2\pi k_0}{\cos\theta}, y, t\right) = \eta(x,y,t), \tag{5.1a}$$

and the second family of wave groups satisfies

$$\eta\left(x+\frac{\pi k_0}{\cos\theta}, y\pm\frac{\pi}{\sin\theta}, t\right) = \eta(x,y,t). \tag{5.1b}$$

Equation (5.1b) demonstrates that the group length of the second family is $\pi k_0/\cos\theta$, equivalent to πL in dimensional terms, since the envelope of the group is obtained by averaging η over y at fixed x and t (which is equivalent to averaging over y or t at fixed $x - \frac{1}{2}t\cos\theta$). Equation (5.1$b$) demonstrates also that at given t the wavetrains in adjoining groups are π out of phase, because $\pi/\sin\theta$ is half the dimensionless wavelength in the y-direction. Wavelength in the y-direction, unlike wavelength in

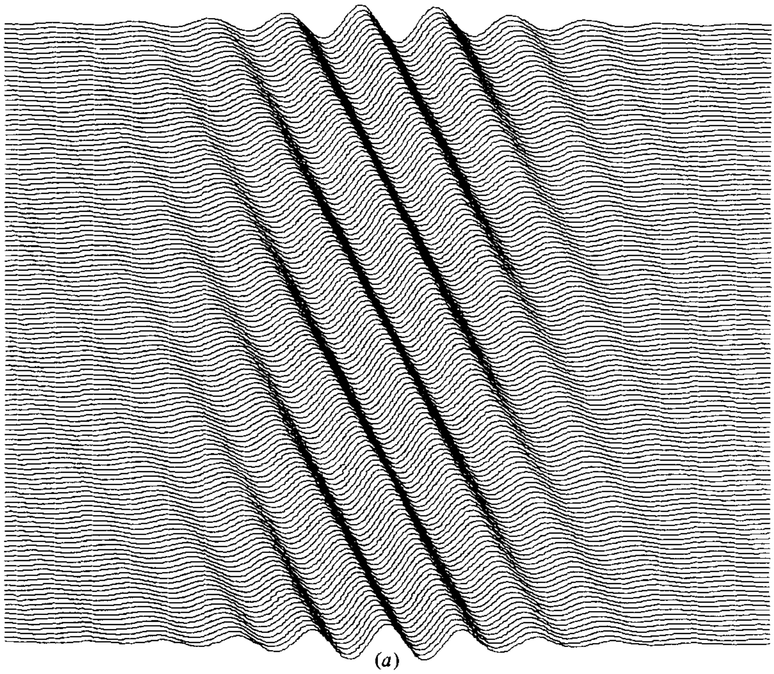

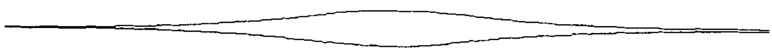

FIGURE 2. (a) One group length of the oblique wave group with parameters $\epsilon = 0.05$, $k_0 = 10$, $\theta = 0.5$, of the first family below the critical angle. Horizontal contraction 10π. (b) Envelope of the above group, which is almost identical with the corresponding envelope solution (dn form) of the nonlinear Schrödinger equation.

the x-direction, remains constant as the wavetrain propagates through the periodic group structure. The difference in wave phase between consecutive groups of the second family may be seen in the crest lines of the example in figure 1 (a) and less clearly in figure 3 (a).

Periodic oblique wave-group solutions from the first family are found for wave to group angles θ up to the critical angle $\tan^{-1}\sqrt{\frac{1}{2}}$. Apparent numerical solutions exist for θ greater than the critical angle, but because their central wavenumbers exceed k_0 by significant ratios, they need rescaling to interpret them correctly. Equation (4.4) shows that the rescaled wave-to-group angle, the actual angle made by the waves in these solutions, lies below the critical angle. Periodic wave-group solutions from the second family are found for wave-to-group angles θ from 0 to $\frac{1}{2}\pi$. The corresponding nonlinear Schrödinger envelope solutions have the same properties, with the elliptic dn solutions occurring only for angles less than the critical angle, but with the elliptic cn and sn solutions (with envelope zeros) occurring for all angles θ from 0 to $\frac{1}{2}\pi$.

An example of an oblique wave group from the first family of wave groups is sketched in figure 2 (a). The parameter values are $\epsilon = 0.05$, $k_0 = 10$, $\theta = 0.5$, with $\alpha = 0.0006$, and one group length is shown. No attempt is made to give perspective to the figure so that wave angles may be measured directly. The envelope of the group is drawn to the same scale in figure 2 (b). The envelope is almost identical with the corresponding elliptic dn solution of the nonlinear Schrödinger equation at these

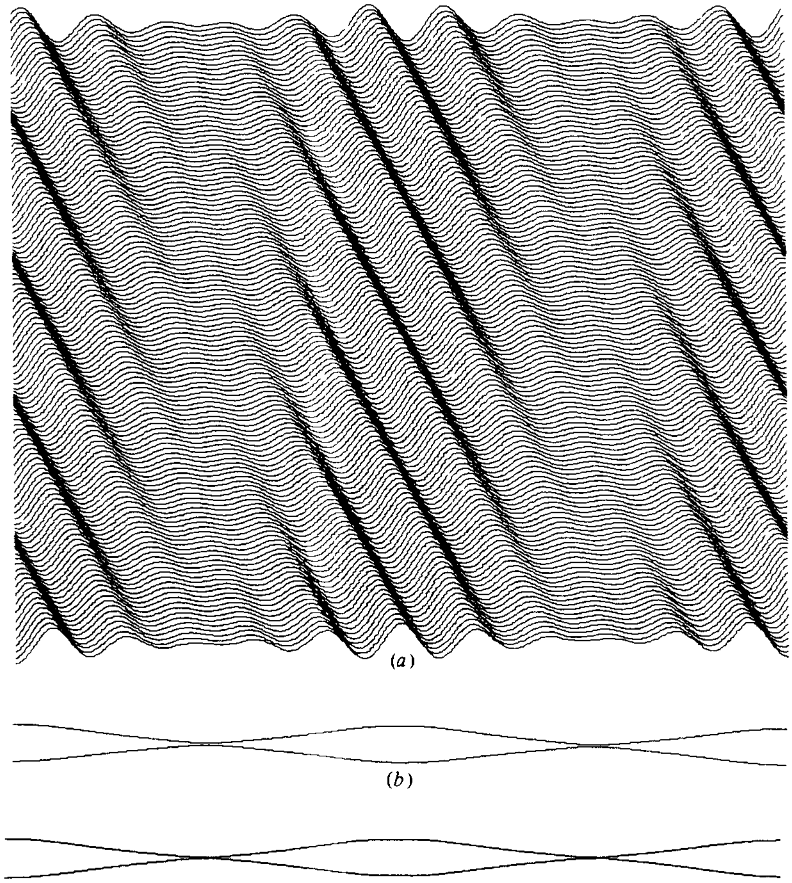

(c)

FIGURE 3. (*a*) Two group lengths of the oblique wave group with parameters $\epsilon = 0.05$, $k_0 = 10$, $\theta = 0.5$, of the second family below the critical angle. Horizontal contraction 10π. (*b*) Envelope of the above groups. Minimum separation of upper and lower envelopes is 0.062 of maximum separation. (*c*) Corresponding envelope solution (cn form) of the nonlinear Schrödinger equation.

parameter values (Hui & Hamilton 1979, figure 2*b*). The full solution (equations 2.4) contains 115 wave components (231 variables) in 7 wavebands $0 \leqslant j \leqslant 6$, the wavenumber range being $1 \leqslant k \leqslant 64$. The maximum Fourier coefficients F_{mn}, G_{mn} not included in the calculation have magnitude 1×10^{-6}. The maximum magnitude of F and G over the 256×16 points used in the final calculation is 2.6×10^{-4}, with a root-mean-square deviation of F and G from zero of 5.5×10^{-5}. (A computer listing of the wave components for all examples may be obtained from the author).

The equivalent example from the second family of wave groups, with $\alpha = 0.0005$, is sketched in figure 3(*a*). Two group lengths are shown so that it may be seen how the waves in the two outer half-groups each differ by π from the waves in the centre group. The envelope of the group is drawn in figure 3(*b*), and the corresponding envelope solution of the nonlinear Schrödinger equation in figure 3(*c*). The two envelopes are almost identical except in the neighbourhood of the envelope zeros of the nonlinear Schrödinger equation, which in the actual envelope are replaced by upper and lower envelope extrema. The nonlinear-Schrödinger-equation solution has the elliptic cn form (Hui & Hamilton 1979, figure 2(*a*)).

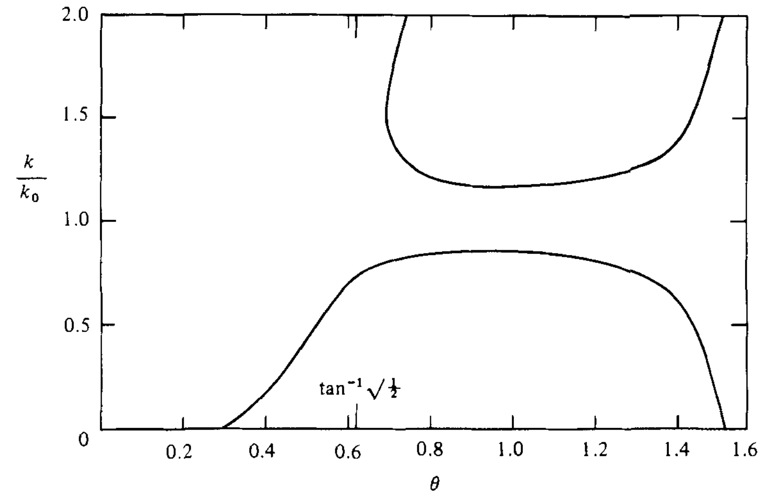

FIGURE 4. Wavenumber ratio for resonance in the dominant waveband.

An example of an oblique wave group of the second family for which the wave-to-group angle θ exceeds the critical angle was sketched in figure 1 (a), with parameter values $\epsilon = 0.05$, $k_0 = 10$, $\theta = \frac{1}{4}\pi$ and $\alpha = 0.0013$. The envelope of the group and the corresponding envelope solutions of the nonlinear Schrödinger equation are sketched in figures 1 (b, c) respectively, and differ only where the envelope zeros are replaced by envelope extrema in the actual wave envelope. The nonlinear Schrödinger equation solution has the elliptic sn form (Hui & Hamilton 1979, figure 3a).

6. Resonance

The nonlinear Schrödinger equation is valid only if the dominant wave components lie in a narrow waveband in two-dimensional wavenumber space. When an oblique wave group has another major peak in wavenumber space, the nonlinear Schrödinger equation fails as a model of the group. A second spectral peak can be expected to occur if a forced or bound wave component of significant magnitude has the same frequency-to-wavenumber relation as do free gravity waves in deep water. This form of resonance is distinct from resonant instabilities of oblique wave-group solutions of the nonlinear Schrödinger equation, because it is a significant resonant contribution to the structure of the oblique wave group itself. When it is present, the nonlinear Schrödinger equation, and perturbations to it, are no longer valid models of the modified oblique wave groups and their stability.

The wavenumber and frequency of one of the forced wave components in the oblique wave group represented by (2.4a) satisfy the linear dispersion relation for deep-water gravity waves when

$$j(1+\alpha-\tfrac{1}{2}\cos^2\theta)+\frac{1}{2}\frac{k}{k_0}\cos^2\theta = \left\{\left(\frac{k}{k_0}\right)^2\cos^2\theta + j\sin\theta)^2\right\}^{\frac{1}{4}}. \tag{6.1}$$

The values of k/k_0 given by this equation are plotted as a function of θ for the dominant waveband $j = 1$ in figure 4. The frequency correction α makes little contribution to these curves, the points being calculated for oblique wave groups with $\epsilon = 0.05$, $k_0 = 10$, when α takes values between 0.0004 and 0.0014 over the range of

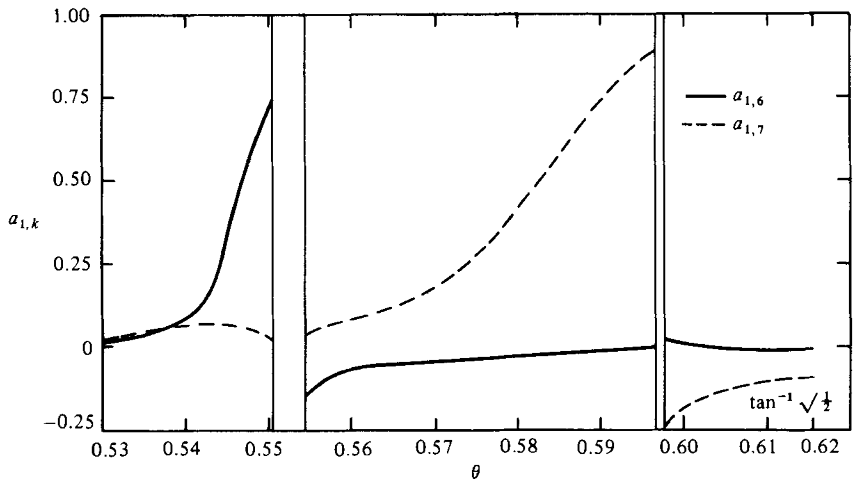

FIGURE 5. Resonant behaviour of the wave amplitudes $a_{1,6}, a_{1,7}$ for oblique wave groups of the first family with $\epsilon = 0.05$, $k_0 = 10$.

θ shown. Resonances in other wavebands ($j = 0, 2, 3, \ldots$) do not occur for values of k/k_0 at which wave components contribute to the oblique wave-group structure.

The points on the resonance curves corresponding to integer values of k indicate values of θ near which oblique wave groups are modified or may not exist because of the resonant generation of one of their wave components. As θ approaches such a value, the resonating wave component increases in magnitude relative to the other wave components, and as the value is crossed the wave component and the Jacobian in Newton's method change sign. This effect is slight for small or large values of k/k_0, but for k/k_0 near 1 the effect becomes significant. The curve in figure 4 indicates that, if k_0 is 10, $a_{1,6}$ is resonant at $\theta = 0.553$ and $a_{1,7}$ is resonant at $\theta = 0.592$.

The amplitudes $a_{1,6}$, $a_{1,7}$ for oblique wave groups of the first family are sketched in figure 5 as functions of θ for a range including resonance. No solutions for oblique wave groups could be found when $0.550 < \theta < 0.555$, where $a_{1,6}$ is resonant. As θ approaches 0.550 from below, the spectral peaks at ($j = 1$, $k = 6$) and ($j = 1$, $k = k_0 = 10$) are of equal magnitude at $\theta = 0.544$, and the resonant peak exceeds the central peak for $0.544 < \theta \leqslant 0.550$. The amplitude $a_{1,6}$ at $\theta = 0.550$ has a magnitude 5 times that of the central amplitude $a_{1,10}$. The actual envelope of the oblique wave group at $\theta = 0.555$, on the upper side of the resonance of $a_{1,6}$, is compared in figure 6 with the corresponding envelope solution of the nonlinear Schrödinger equation. The figure illustrates the modification to the envelope shape which is caused by the resonating wave component. The amplitude $a_{1,7}$ rises more strongly towards resonance than does $a_{1,6}$, with the resonant peak at ($j = 1$, $k = 7$) exceeding the central peak for $0.572 < \theta \leqslant 0.596$. The amplitude $a_{1,7}$ at $\theta = 0.596$ has a magnitude 32 times that of the central amplitude $a_{1,10}$. No solutions could be found for $0.596 < \theta \leqslant 0.598$. Nonlinear modification due to the large amplitude is the probable reason for this discontinuity in $a_{1,7}$ occurring beyond the value of linear resonance deduced from (6.1).

The amplitude $a_{1,7}$ for oblique wave groups of the second family is sketched in figure 7 as a function of θ for the same range as in figure 5 (the amplitude $a_{1,6}$ is zero for oblique wave groups of the second family). The upper curve describes the approach to resonance from below on a solution branch which began at $\theta = 0$. The

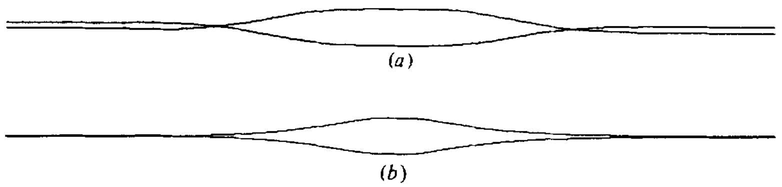

FIGURE 6. (*a*) Envelope of the oblique wave group with parameters $\epsilon = 0.05$, $k_0 = 10$, $\theta = 0.555$, of the first family. Minimum separation of upper and lower envelopes is 0.016 of maximum separation. Horizontal contraction 10π. (*b*) Corresponding envelope solution (dn form) of the nonlinear Schrödinger equation.

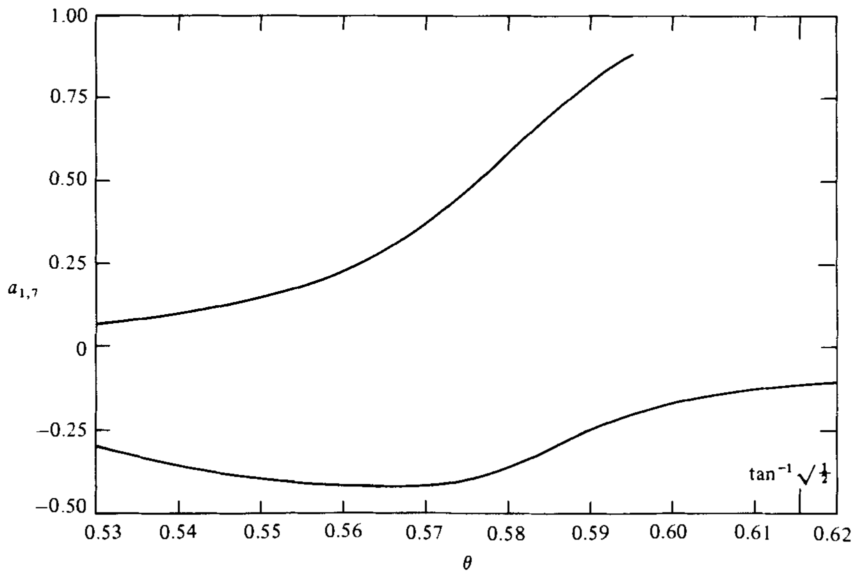

FIGURE 7. Resonant behaviour of the wave amplitude $a_{1,7}$ for oblique wave groups of the second family with $\epsilon = 0.05$, $k_0 = 10$.

resonant peak at ($j = 1$, $k = 7$) exceeds the two central peaks ($j = 1$, $k = 9$ and 11) for $0.566 < \theta \leqslant 0.595$. The amplitude $a_{1,7}$ at $\theta = 0.595$ has a magnitude 10 times greater than either of the two central amplitudes $a_{1,9}$ or $a_{1,11}$. The lower curve, if continued beyond the figure for values of θ above the critical angle, may be followed to $\theta = 0.707$, where it terminates because the amplitude $a_{1,15}$ reaches a positive resonance maximum. As θ is decreased below the critical angle, the lower curve describes the approach of the amplitude $a_{1,7}$ towards resonance from above. It then merges continuously into a curve for a solution branch dominated by $a_{1,7}$ and $a_{1,11}$, which is better interpreted in terms of its conjugate branch at angles above the critical angle (§4). The oblique wave-group solution with $a_{1,7}$ on the lower curve at $\theta = 0.53$, with $\epsilon = 0.05$, $k_0 = 10$, for example, is conjugate to one at $\theta = 0.70$ with $\epsilon = 0.4$, $k_0 = 6.92$. Reference to figure 4 shows that there are three values for linear resonance at $\theta = 0.70$, namely $k/k_0 = 0.8$, 1.4 or 1.6, equivalent to $k = 5.5$, 9.7 or 11.1 when $k_0 = 6.92$. A better interpretation of the numerical solution at $\theta = 0.53$ on the lower curve of figure 7 is that the actual solution has a wave-to-group angle $\theta = 0.70$ corresponding to a central peak near ($j = 1$, $k = k_0 = 7$) and a resonant peak near ($j = 1$, $k = 11$).

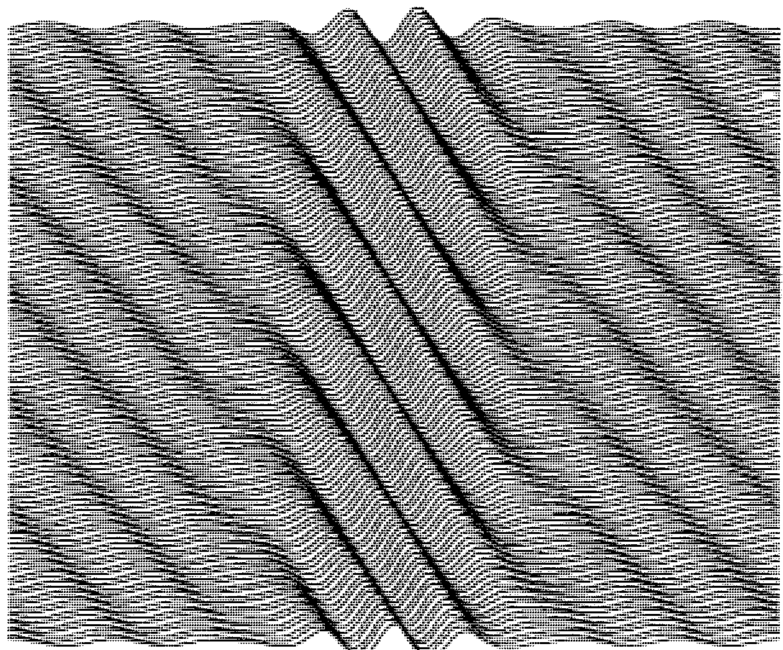

(a)

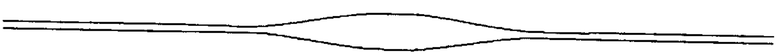

(b)

FIGURE 8. (a) One group length of the oblique wave group with parameters $\epsilon = 0.05$, $k_0 = 10$, $\theta = \tan^{-1}\sqrt{\frac{1}{2}}$ of the first family at the critical angle. Horizontal contraction 10π. (b) Envelope of the above group. Minimum separation of upper and lower envelopes is 0.154 of maximum separation.

The multiple linear resonances near $\theta = 0.7$ in figure 4 have no relevance to oblique wave groups of the first family, since these groups do not exist for angles greater than the critical angle. They are relevant to the second family, and produce multiple solution branches. At $\theta = 0.68$, for instance, three distinct solution branches have been found, each of which displays resonant behaviour of different sets of wave components. The amplitudes $a_{1,11}$, $a_{1,13}$, $a_{1,15}$, $a_{1,17}$ all pass through resonance near $\theta = 0.68$ in oblique wave groups for which $k_0 = 10$. The occurrence of multiple oblique wave-group solutions with steady envelopes for wave-to-group angles near $\theta = 0.7$ suggests that it may be difficult to generate or observe isolated periodic oblique wave groups with steady envelopes near this angle. It is expected rather that the envelopes of the oblique wave groups remain unsteady with a continuing interchange of energy between resonating wave components.

7. Oblique wave groups at the critical angle

Oblique wave-group solutions of the nonlinear Schrödinger equation have permanent envelopes which satisfy (3.4), an equation which is singular at the critical angle $\theta = \tan^{-1}\sqrt{\frac{1}{2}} = 0.6155$. Hui & Hamilton (1979) found oblique wave-group solutions of the nonlinear Schrödinger equation at the critical angle for which the envelope of the wave group is arbitrary. These solutions satisfy locally the nonlinear dispersion

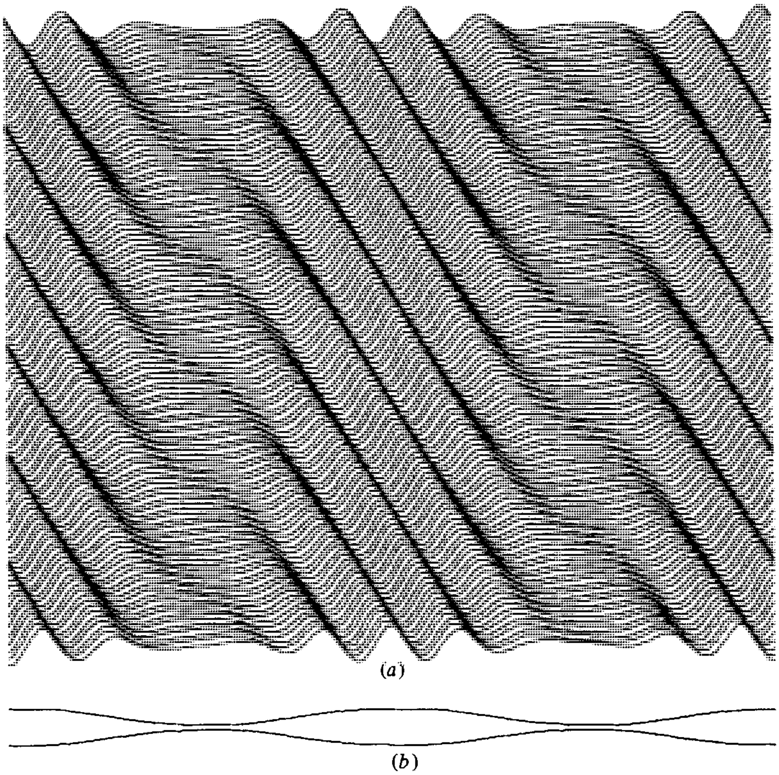

FIGURE 9. (*a*) Two group lengths of the oblique wave group with parameters $\epsilon = 0.05$, $k_0 = 10$, $\theta = \tan^{-1}\sqrt{\frac{1}{2}}$ of the second family at the critical angle. Horizontal contraction 10π. (*b*) Envelope of the above groups. Minimum separation of upper and lower envelopes is 0.136 of maximum separation.

relation for a Stokes wavetrain. In contrast, the oblique wave groups calculated by the present method as solutions of equations (2.1) at the critical angle have the same form as oblique wave groups near the critical angle. Resonating wave components contribute significantly to the oblique wave-group structure in all examples calculated at or near the critical angle, implying that the nonlinear Schrödinger equation is not a valid model for oblique wave groups in this region.

An oblique wave group of the first family at the critical angle is sketched in figure 8(*a*), and its envelope is drawn to the same scale in figure 8(*b*). The parameters are $\epsilon = 0.05$, $k_0 = 10$, $\theta = \tan^{-1}\sqrt{\frac{1}{2}}$, with $\alpha = 0.0008$. The wave components with magnitudes exceeding 10^{-4} are tabulated in the Appendix. The spectrum of the group has two equal peaks at ($j = 1$, $k = 8$) and ($j = 1$, $k = 11$). The existence of two equal peaks in the spectrum confirms that the nonlinear Schrödinger equation is not a valid model equation here. The sketch of the oblique wave group in figure 8(*a*) shows eight wavelengths per group length in the x-direction across the complete group length, consistent with the resonance associated with the first spectral peak. The solution contains 145 harmonics (291 variables) in 7 wavebands $0 \leqslant j \leqslant 6$, the wavenumber range being $1 \leqslant k \leqslant 67$. The maximum Fourier coefficients F_{mn}, G_{mn} not included have magnitude 1×10^{-6}, the maximum magnitude of F and G over the 256×16 points used in the final calculation is 3.0×10^{-4}, with a root-mean-square deviation of F and G from zero of 6.0×10^{-5}.

An oblique wave group of the second family at the critical angle is sketched in figure 9(*a*), and its envelope in figure 9(*b*). The parameters are $\epsilon = 0.05$, $k_0 = 10$,

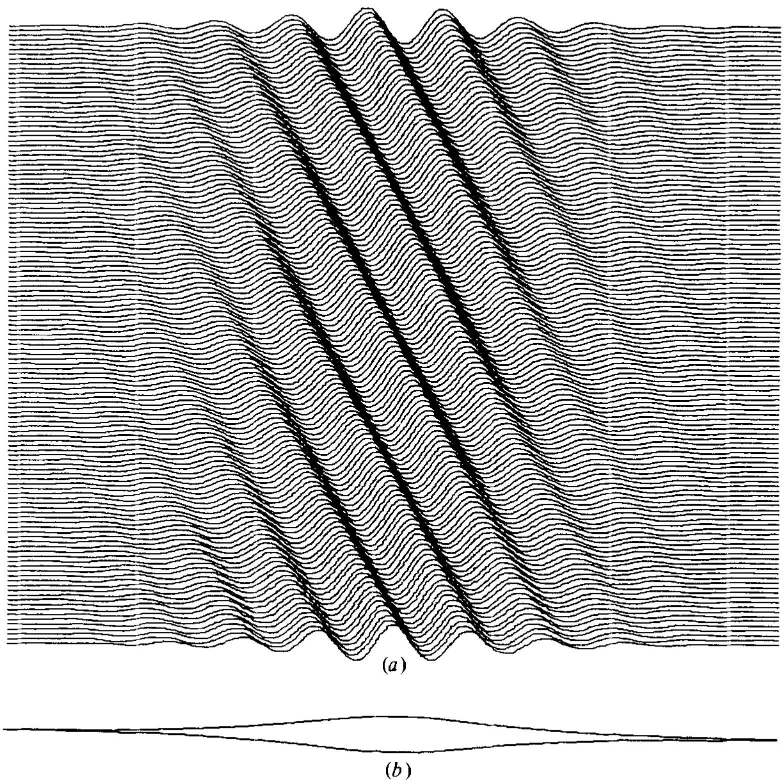

FIGURE 10. (a) Central fifth of one group length of the oblique wave group with parameters $\epsilon = 0.05$, $k_0 = 50$, $\theta = 0.5$, of the first family. Horizontal contraction 10π. (b) Envelope of the above part of the group, which is almost identical with the corresponding envelope solution (sech form) of the nonlinear Schrödinger equation.

$\theta = \tan^{-1}\sqrt{\frac{1}{2}}$, with $\alpha = 0.0009$. The wave components with magnitudes exceeding 10^{-4} are tabulated in the Appendix. The amplitude $a_{1,7}$ in this example is found on the lower curve of figure 7 at the critical angle. The amplitude $a_{1,11}$ has a magnitude 1.5 times the other central amplitude $a_{1,9}$ because this wave component lies near resonance (figure 4) at the critical angle. Nearness to resonance on the upper curve of figure 4 dominates nearness to resonance on the lower curve of figure 4 for this part of the solution branch.

8. Solitary oblique wave groups

The nonlinear Schrödinger equation has two solutions describing solitary oblique wave groups of permanent envelope. These are the envelopes of sech shape and of tanh shape (Hui & Hamilton 1979, figures 2c, 3b). The envelope of sech shape occurs in the large group-length to wavelength limit for periodic oblique wave groups with wave-to-group angles less than the critical angle. At finite group lengths for angles in this region, the dn envelope solutions do not have envelope zeros, while the cn solutions do have envelope zeros with a phase discontinuity of π at each zero. The limiting processes differ therefore for the two types of solution. This difference is reflected in the two families of periodic oblique wave groups calculated by the present method. The envelopes of the two families at wave to group angles less than the critical angle tend to the same form unless resonating wave components are

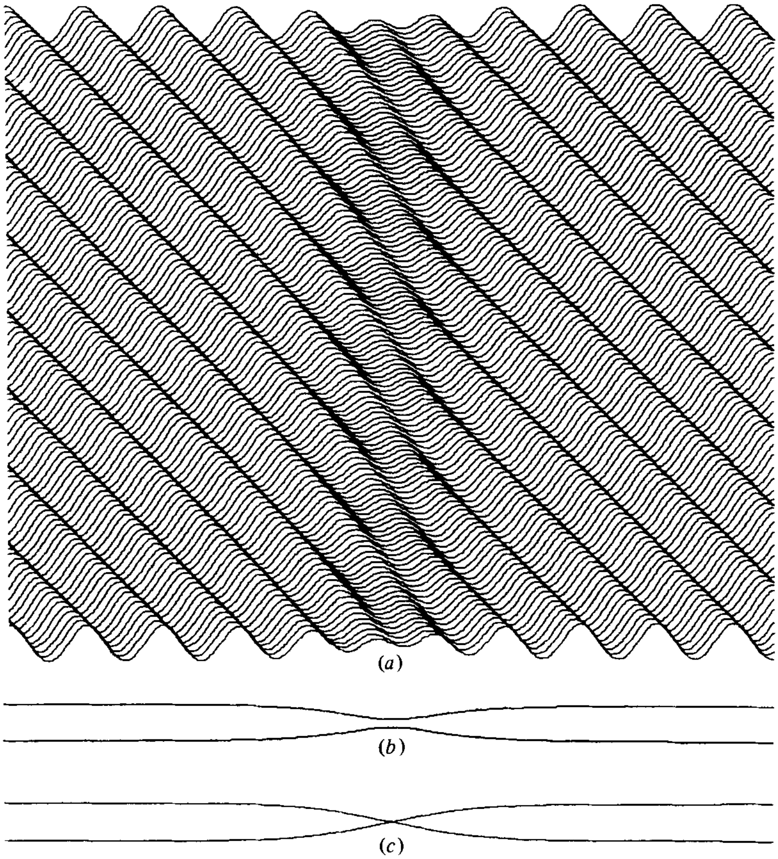

FIGURE 11. (*a*) One fifth of one group length of the oblique wave group with parameters $\epsilon = 0.05$, $k_0 = 100$, $\theta = \frac{1}{4}\pi$, of the second family. Horizontal contraction 10π. (*b*) Envelope of the above part of the group. Minimum separation of upper and lower envelopes is 0.208 of maximum separation. (*c*) Corresponding envelope solution (tanh form) of the nonlinear Schrödinger equation.

significant. However, in the limiting process, the waves in each group are in phase for the first family, but the waves in consecutive groups are π out of phase for the second family. The envelope of tanh shape occurs in the large group-length to wavelength limit with wave to group angles greater than the critical angle.

The central ten wavelengths of the oblique wave group with parameters $\epsilon = 0.05$, $k_0 = 50, \theta = 0.5, \alpha = 0.0006$ are sketched in figure 10 (*a*), and the envelope of this part of the group is drawn in figure 10 (*b*). The group length is completed by 20 wavelengths of nearly zero wave height on each side of the part shown. The amplitudes $a_{1,21}$, $a_{1,22}$ have small resonant peaks, with phases such that $a_{1,21}$ is negative and $a_{1,22}$ is positive, corresponding to the linear resonance for the angle $\theta = 0.5$ (figure 4) at $k/k_0 = 4.20$, equivalent to $k = 21$ with $k_0 = 50$. This resonance is sufficiently small that the envelope of the group in figure 10 (*b*) almost coincides with the corresponding envelope solution of the nonlinear Schrödinger equation.

Attention is drawn to the close resemblance between figures 2 and 10. The complete group length illustrated in figure 2 is almost identical with the partial group length at the same wave-to-group angle illustrated in figure 10.

Ten wavelengths of the oblique wave group with parameters $\epsilon = 0.05$, $k_0 = 100$, $\theta = \frac{1}{4}\pi$, $\alpha = 0.0012$ are sketched in figure 11 (*a*), the envelope of this part of the group is drawn in figure 11 (*b*), and the part of the corresponding envelope solution of the nonlinear Schrödinger equation is drawn in figure 11 (*c*). One tenth of the double group length centred on either of the two envelope minima (see figure 1) is shown in figure 11, with ten wavelengths included. The remainder of the group consists of 20 wavelengths of uniform wave height on each side of the part shown in the figure. This form of solitary wave group solution of the nonlinear Schrödinger equation is referred to as the dark soliton by Peregrine (1983) and others. The linear resonance at $\theta = \frac{1}{4}\pi$ (figure 4) contributes to the amplitudes of the two central wave components $a_{1,9}$ and $a_{1,11}$. It may be seen on comparing figures 11 (*b*) and 11 (*c*) how the zero of the nonlinear Schrödinger envelope solution is replaced by upper and lower envelope extrema in the actual oblique wave group.

9. Discussion

There are two points of wider interest in the present calculations of periodic oblique wave groups of permanent envelope. These concern the role of resonant interactions between wave components, and the absence of envelope zeros in the calculated wave groups.

A deficiency has been confirmed in the applicability of the nonlinear Schrödinger equation to slowly varying water-wave motion in two horizontal dimensions. The problem lies with the assumption in this equation that the water wave spectrum has a narrow peak in two-dimensional wavenumber space. The possibility exists that the resonant forcing of certain wave components in two horizontal dimensions generates further spectral peaks, a property demonstrated originally by Phillips (1960). Solutions calculated from the nonlinear Schrödinger equation which are to be applied to water-wave motion must be tested to determine whether any of the significant wave components in the solution satisfy the linear dispersion relation. If there are wave components with this property, such a solution may be modified significantly by resonating wave components.

The nonlinear Schrödinger equation has solutions with envelope zeros (Hui & Hamilton 1979, Peregrine 1983). An envelope zero introduces an additional zero into the slowly varying wavetrain, which changes locally the horizontal lengthscales and raises doubts about the local applicability of the nonlinear Schrödinger equation. It is therefore of interest that the envelope zeros in oblique wave-group solutions of the nonlinear Schrödinger equation are replaced by positive minimum envelope separations in all oblique wave groups calculated here, with no additional zeros in the wavetrain. Recent measurements by Melville (1983) show that rapid variations in wave phase occur near the minima of wave amplitude in an evolving slowly varying Stokes wavetrain. Melville's observations were made at larger wave slopes ($0.23 \leqslant \epsilon \leqslant 0.29$) than that used here ($\epsilon = 0.05$), with an envelope that is unsteady, and are therefore not inconsistent with the properties calculated here.

This investigation has demonstrated a straightforward method for the numerical calculation of solutions of the equations for irrotational gravity wave motion in deep water. The method has generalizations to water of finite depth, to short waves with significant surface tension, and to other forms of water-wave motion. Properties are found for the full nonlinear theory without recourse to model nonlinear equations such as the Schrödinger equation or the Zakharov equation, or to perturbation expansions in the wave-slope parameter.

Appendix

Wave components with magnitudes exceeding 10^{-4} for the oblique wave-group example of the first family whose wave-to-group angle is the critical angle (§7):

a_{jk}

$j = 0,\ k = 1\text{–}7$

−0.0002	−0.0003	−0.0003	−0.0002	−0.0001	—	—	

$j = 1,\ k = 4\text{–}20$

−0.0002	−0.0016	−0.0097	−0.0922	0.2072	0.1639	0.1911	0.2001
0.1527	0.0871	0.0427	0.0194	0.0084	0.0035	0.0014	0.0006
0.0002							

$j = 2,\ k = 15\text{–}29$

−0.0008	0.0002	0.0007	0.0016	0.0028	0.0037	0.0040	0.0037
0.0031	0.0024	0.0016	0.0010	0.0006	0.0003	0.0002	

$j = 3,\ k = 30\text{–}34$

0.0001	0.0001	0.0001	0.0001	0.0001

b_{jk}

$j = 0,\ k = 1\text{–}7$

−0.0058	−0.0049	−0.0034	−0.0019	−0.0008	−0.0003	−0.0001

$j = 1,\ k = 4\text{–}20$

−0.0002	−0.0018	−0.0112	−0.1023	0.2219	0.1696	0.1911	0.1936
0.1432	0.0793	0.0377	0.0167	0.0070	0.0028	0.0011	0.0004
0.0002							

$j = 2,\ k = 15\text{–}29$

—	—	—	—	—	—	—	—
—	—	—	—	—	—	—	—

$j = 2,\ k = 30\text{–}34$

—	—	—	—	—

Wave components with magnitudes exceeding 10^{-4} for the oblique wave-group example of the second family whose wave-to-group angle is the critical angle (§7):

a_{jk}

$j = 0,\ k = 2\text{–}8$ even

−0.0007	−0.0003	—	—

$j = 1,\ k = 3\text{–}19$ odd

0.0002	0.0017	−0.1149	0.3198	0.4911	0.2263	0.0438
0.0054	0.0003					

$j = 2,\ k = 14\text{–}30$ even

0.0003	−0.0015	−0.0001	0.0066	0.0100	0.0071	0.0029
0.0008	0.0002					

$j = 3,\ k = 31\text{–}37$ odd

0.0002	0.0003	0.0003	0.0002

b_{jk}

$j = 0,\ k = 2\text{–}8$ even

−0.0110	−0.0022	0.0002	0.0001

$j = 1,\ k = 3\text{–}19$ odd

0.0002	0.0021	−0.1275	0.3307	0.4751	0.2058	0.0377
0.0044	0.0003					

$j = 2$, $k = 14$–30 even

—	—	—	—	—	—	—
—	—					

$j = 3$, $k = 31$–37 odd

—	—	—	—

The complete listing of the wave components for these and the other examples may be obtained from the author.

REFERENCES

BRYANT, P. J. 1983 Cyclic gravity waves in deep water. *J. Austral. Math. Soc.* B **25**, 2–15.

HUI, W. H. & HAMILTON, J. 1979 Exact solutions of a three-dimensional nonlinear Schrödinger equation applied to gravity waves. *J. Fluid Mech.* **93**, 117–133.

LIGHTHILL, J. 1978 *Waves in Fluids*. Cambridge University Press.

McLEAN, J. W., MA, Y. C., MARTIN, D. U., SAFFMAN, P. G. & YUEN, H. C. 1981 Three-dimensional instability of finite-amplitude water waves. *Phys. Rev. Lett.* **46**, 817–820.

MELVILLE, W. K. 1983 Wave modulation and breakdown. *J. Fluid Mech.* **128**, 489–506.

PEREGRINE, D. H. 1983 Water waves, nonlinear Schrödinger equations and their solutions. *J. Austral. Math. Soc.* B **25**, 16–43.

PHILLIPS, O. M. 1960 On the dynamics of unsteady gravity waves of finite amplitude. Part 1. The elementary interactions. *J. Fluid Mech.* **9**, 193–217.

ZAKHAROV, V. E. 1968 Stability of periodic waves of finite amplitude on the surface of a deep fluid. *Zh. Prikl. Mekh. Tekh. Fiz.* **9**, 86–94 (*J. Appl. Mech. Tech. Phys.* **2**, 190–194).